

available at www.sciencedirect.com
journal homepage: www.europeanurology.com



Letters to the Editor NOT referring to a recent journal article

High-Resolution Magnetic Resonance Imaging of Prostatectomy Specimens: A Promising Tool for Virtual Histology

There is currently a wide range of opinion on the role of diagnostic imaging in prostate cancer (PCa). Approaches to the problem vary throughout the world [1]. Amid the debate there is a consensus that magnetic resonance imaging (MRI) is the most useful imaging modality, and since there are many physical mechanisms that produce image contrast via MRI, a large body of work has been published in this area over many years [2–8]. However, current MRI-based imaging still has suboptimal resolution relative to the important morphologic constructs of the gland, often leading to low sensitivity for the location and grade of PCa [4]. The role of MRI in selection of patients for active surveillance, focal therapy, or nerve-sparing surgery remains controversial. To circumvent this problem, over the past two decades, multiparametric MRI has been developed [3,5]. Currently, multiparametric MRI has been established as a standard in clinical use and includes diffusion imaging and dynamic contrast-enhanced imaging. Still, no specific palette of methods has been generally agreed upon for a diagnostic workup.

We investigated the feasibility of ex vivo 7.0 tesla MRI of the human prostate to elucidate features of the prostate gland that are currently beyond the capabilities of clinical imaging, but whose visualisation is ultimately necessary for the discussion of prostate pathologies within the context of functional and structural organ components. We did an initial, prospective, experimental study on unfixed, excised, human prostate specimens obtained from either organ donors or patients who underwent radical prostatectomy ($n = 12$) from March 2011 to October 2011 under an institutional review board-approved protocol that included signed informed consent.

Whole glands were first cut and quartered to achieve 5-mm thick sections. The sections were placed into a standard pathology cassette with inside dimensions of $30 \times 27 \times 5$ mm. Cassettes were immersed in a solution of 0.9% saline and 1% gadolinium-diethylenetriamine pentaacetic acid (Gd-DTPA) for approximately 1 h prior to imaging. Images were acquired on a Bruker Biospec 7.0-T 30-cm bore MRI system (Bruker Biospin, Billerica, MA, USA) equipped with B-GA 12S gradient coils rated at 450 mT/m. An apparatus was constructed in house to contain the pathology

cassette and included a home-built, parallel-wound, solenoid resonator for signal transmission and reception [9]. Turbo spin echo and gradient echo acquisition techniques were applied to the specimens. The turbo spin echo method included a 5.5×5.5 -cm field of view, 75.8 ms effective echo time, a 2-s sequence repetition time, 1024×1024 matrix size, 0.50-mm slice thickness, an echo train length of 12, and 14 excitations. This sequence had a scan time of 40 min and a spatial resolution of $54 \times 54 \times 500 \mu\text{m}^3$. A three-dimensional, fast low-angle shot (FLASH) gradient echo sequence was used for the highest resolution, overnight, specimen imaging with a 6.0×6.0 -cm field of view, 13-ms echo time, 26.3-ms sequence repetition time, $1024 \times 1024 \times 192$ matrix size, 15° flip angle, 60- μm slice thickness, and six excitations. This sequence had a scan time of 8 h and 36 min, a spatial resolution of $60 \times 60 \times 60 \mu\text{m}^3$, and allowed for full coverage of the 5-mm thick specimen, which aided subsequent registration with histology. Finally, the corresponding tissues were subjected to haematoxylin and eosin (H&E) staining for histologic confirmation, using 5- μm thick slices from the 5-mm thick sections used for imaging.

A spin echo image of a sectioned specimen is presented in Figure 1A. There is both gross and specific registration of the MRI and H&E images as shown in Figures 1B–D. In particular, the microanatomy of intraprostatic tissue is well defined on MRI. Individual ducts are clearly visible, along with the presence of intraductal concretions.

A specimen from an organ donor is presented in Figure 1E. Note that at this resolution it is possible to discern specific aggregations of cells, as confirmed in the corresponding H&E slide of Figure 1F. In addition, dark striations in Figure 1E are suggestive of microvasculature, which was confirmed via histology. When processed as a minimum-intensity projection image through a stack of 40 slices obtained from the three-dimensional gradient echo, the result was the angiogram shown in Figure 1G. Conversely, a maximum-intensity projection through the same stack provided the ductogram of Figure 1H. A specimen with confirmed PCa is shown in Figure 1I–K. At a spatial resolution of $60 \times 60 \times 90 \mu\text{m}^3$, PCa is visible with a Gleason score of 6 (3 + 3).

As mentioned previously, there is a well-known, large array of methods for parametric imaging that has already been applied to the prostate, and several studies specifically address comparisons with histology [10–12]. As spatial resolution improves it should be possible to separately

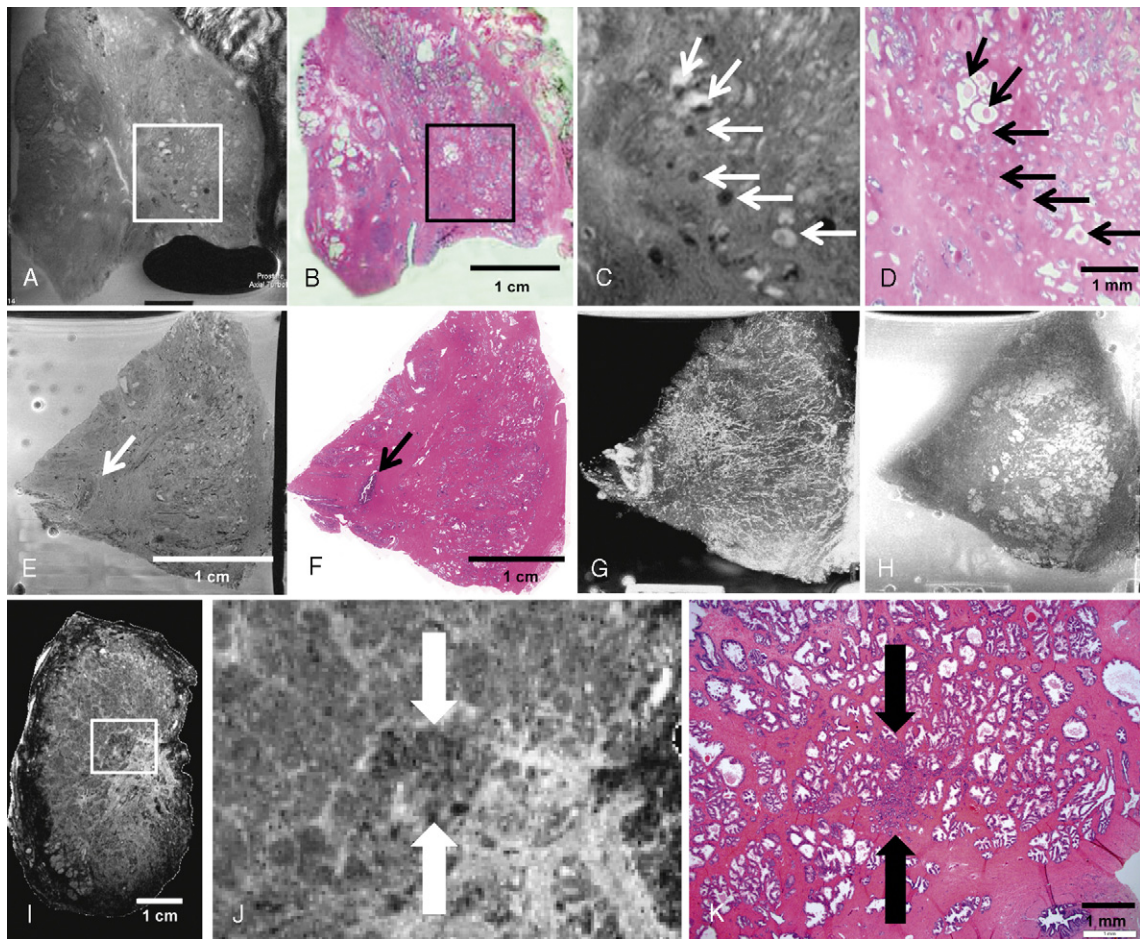


Fig. 1 – Sectioned radical prostatectomy specimens. (A) Spin echo magnetic resonance image (MRI) at a spatial resolution of $54 \times 54 \times 500 \mu\text{m}^3$. (B) Histologic preparation of the specimen in **Figure 1A**. (C, D) Expanded views of the areas within the boxes on **Figure 1A** and **1B** exhibiting intraductal concretions (arrows). (E) Gradient echo image of a specimen obtained from an organ donor at a resolution of $60 \times 60 \times 60 \mu\text{m}^3$. At this resolution it is possible to discern specific aggregations of cells (arrows), as confirmed in the corresponding slide stained with haematoxylin and eosin (F). (G) Angiogram and (H) ductogram composed from 40 contiguous MRI slices. (I) Gradient echo MRI at a resolution of $60 \times 60 \times 90 \mu\text{m}^3$. (J) Zoomed area of **Figure 1I** showing an area of prostate cancer, as confirmed in **Figure 1K**. The Gleason score was 6 (3 + 3).

characterise stroma, ducts, vasculature, concretions, and carcinoma by virtue of T_1 or T_2 relaxation times, diffusion coefficients, as well as dynamic contrast enhancement and spectral characteristics.

Figure 1G is, to our knowledge, the first magnetic resonance angiogram of prostate tissue. This type of presentation may offer opportunities for further study of PCa, such as whether the disruption of normal vascular patterns correlates with the size or grade of tumour. It may also be useful to study whether the vascular density within a tumour correlates with clinical behaviour, as quantification of vascular density from the image would be straightforward.

Given the rapid pace of advancement of radiologic imaging techniques, it is reasonable to speculate that in vivo clinical images will begin to approach the histologic frontier in the not too distant future. It does appear evident that radiologists will evaluate forms of image contrast considerably different from those now accepted in order to properly interpret true high-resolution images of the prostate gland. In addition, as spatial resolution in MRI

continues to improve, virtual histology may become a tool for the practicing pathologist, not only as an aid in diagnosing PCa but also to provide information that complements routine histologic findings, thereby providing clinicians and patients with a more complete understanding of the disease. Finally, the use of virtual histology may provide spatial mapping of cancer in the intact gland and obviate the need for multiple biopsies in the process of deciding on focal versus radical therapeutic strategies.

Conflicts of interest: The authors have nothing to disclose.

References

- [1] Hricak H, Choyke PL, Eberhardt SC, Leibel SA, Scardino PT. Imaging prostate cancer: a multidisciplinary perspective. *Radiology* 2007; 243:28–53.
- [2] Dickinson L, Ahmed HU, Allen C, et al. Magnetic resonance imaging for the detection, localisation, and characterisation of prostate cancer: recommendations from a European Consensus Meeting. *Eur Urol* 2011;59:477–94.

- [3] Delongchamps NB, Rouanne M, Flam T, et al. Multiparametric magnetic resonance imaging for the detection and localization of prostate cancer: combination of T2-weighted, dynamic contrast-enhanced and diffusion-weighted imaging. *BJU Int* 2011;107:1411–8.
- [4] Villers A, Puech P, Leroy X, Biserte J, Fantoni J-C, Lemaitre L. Dynamic contrast-enhanced MRI for preoperative identification of localised prostate cancer. *Eur Urol Suppl* 2007;6:525–32.
- [5] Carroll PR, Coakle FV, Kurhanewicz J. Magnetic resonance imaging and spectroscopy of prostate cancer. *Rev Urol* 2006;8(Suppl 1):S4–10.
- [6] Ahmed HU, Kirkham A, Arya M, et al. Is it time to consider a role for MRI before prostate biopsy? *Nat Rev Clin Oncol* 2009;6:197–206.
- [7] Sciarra A, Barentsz J, Bjartell A, et al. Advances in magnetic resonance imaging: how they are changing the management of prostate cancer. *Eur Urol* 2011;59:962–77.
- [8] Barentsz JO, Richenberg J, Clements R, et al. ESUR prostate MR guidelines 2012. *Eur Radiol* 2012;22:746–57.
- [9] Bath KG, Voss HU, Jing D, et al. Quantitative intact specimen magnetic resonance microscopy at 3.0 T. *Magn Reson Imaging* 2009;27:672–80.
- [10] Zhan Y, Feldman M, Tomaszewski J, Davatzikos C, Shen D. Registering histological and MR images of prostate for image-based cancer detection. *Med Image Comput Comput Assist Interv* 2006;9:620–8.
- [11] Turkbey B, Mani H, Shah V, et al. Multiparametric 3T prostate magnetic resonance imaging to detect cancer: histopathological correlation using prostatectomy specimens processed in customized magnetic resonance imaging based molds. *J Urol* 2011;186:1818–24.
- [12] Fan X, Haney CR, Agrawal G, et al. High-resolution MRI of excised human prostate specimens acquired with 9.4T in detection and identification of cancers: validation of a technique. *J Magn Reson Imaging* 2011;34:956–61.

Matthieu Durand^{a,d,*}
 Brian D. Robinson^{a,b}
 Eric Aronowitz^c
 Ashutosh K. Tewari^{a,†}
 Douglas J. Ballon^{c,†}

^aDepartment of Urology, Institute of Prostate Cancer, and Lefrak Center for Robotic Surgery, Weill Medical College of Cornell University, New York, NY, USA

^bDepartment of Pathology and Laboratory Medicine, Weill Medical College of Cornell University, New York, NY, USA

^cDepartment of Radiology, Weill Medical College of Cornell University, New York, NY, USA

^dDepartment of Urology, Nice University Hospital, Nice, France

[†]Equally contributing senior authors.

*Corresponding author. Nice University Hospital, Urologie, Hôpital ARCHET 2, 151 Route Saint Antoine Ginestière, BP 79, 06202 Nice Cedex 3, France.
 E-mail address: matsdurand@yahoo.fr (M. Durand).

August 10, 2012

Published online ahead of print on August 18, 2012

<http://dx.doi.org/10.1016/j.eururo.2012.08.023>

Uptake of Laparoscopic Radical Nephroureterectomy in France: A 2003–2011 National Practice Report

Radical nephroureterectomy (RNU) with excision of the bladder cuff is the treatment of choice for high-risk non-invasive and invasive upper tract urothelial carcinoma [1]. With the diffusion of laparoscopy over the last two decades, laparoscopic RNU (LNU) has gained increasing popularity compared to open RNU (ONU).

Recently, a propensity-score-matched analysis [2] and a systematic review (with cumulative analysis) of available comparative studies [3] suggested that some intra- and perioperative outcomes were more favorable in patients treated with LNU compared with ONU. Specifically, LNU patients were less likely to require a blood transfusion and/or to experience intraoperative complications and had a shorter length of stay. These considerations could be important from a patient's perspective as well as a system's perspective (eg, resource allocation, cost effectiveness). In addition to the potentially improved perioperative outcomes, LNU seems noninferior to ONU with regard to midterm oncologic outcomes [3,4]. Although there are no well-powered prospective trials evaluating the long-term outcomes of LNU versus ONU, LNU has been widely adopted by the urologic community.

In the present study, we aimed to report the national practice patterns of LNU and ONU in France, relying on the

data from the Programme de médicalisation des systèmes d'information (PMSI) database from the French national health insurance program. We obtained yearly numbers of RNUs performed between 2003 and 2011 from the French national PMSI database. All performed surgical interventions are registered in France regardless of the health care center, making the PMSI database reliable and complete. Data are anonymized and are regularly controlled by a national agency.

The total number of RNUs remained consistent between 2003 and 2011, with approximately 1800 RNUs performed per year. The number of LNUs increased slowly but steadily until it surpassed the number of ONUs in 2010 (Fig. 1). Interestingly, 45% of the RNUs in 2011 were still performed by the open approach. The rates of LNU uptake in public (academic centers) and private-practice hospitals were similar, with private-practice hospitals showing a slightly faster uptake. In 2011, the public hospitals performed 45% of the RNUs, and 55% of the RNUs in France were performed in private-practice hospitals. No difference was reported between geographic regions in France, as laparoscopic devices have been widely distributed throughout the country.

Despite a growing popularity of LNU, ONU is still commonly performed in France. In 2010, LNU became the preferred approach for RNU in France. Currently, the rates of LNU and ONU are similar for public and private hospitals.